

Supplementary Information

Strong extended SWIR cavity resonances in a single GeSn nanowire

Youngmin Kim^{1†}, Simone Assali^{2†}, Hyo-Jun Joo¹, Sebastian Koelling², Melvina Chen¹, Lu Luo², Xuncheng Shi¹, Daniel Burt¹, Zoran Ikonic³, Donguk Nam^{1*} and Oussama Moutanabbir^{2*}

¹School of Electrical and Electronic Engineering, Nanyang Technological University, 50 Nanyang Avenue, Singapore 639798, Singapore

²Department of Engineering Physics, École Polytechnique de Montréal, C.P. 6079, Succ. Centre-Ville, Montréal, Québec H3C 3A7, Canada

³School of Electrical and Electronic Engineering, University of Leeds, Leeds LS2 9JT, UK

[†]These authors contributed equally to this work.

*E-mail: dnam@ntu.edu.sg, oussama.moutanabbir@polymtl.ca

Table of Content

Note 1. Nanowire transfer procedure

Note 2. Raman analysis on nanowires before and after transfer process

Note 3. Optical mode confinement of as-grown and transferred nanowires

Note 4. Comparison between simulated and experimental cavity resonances

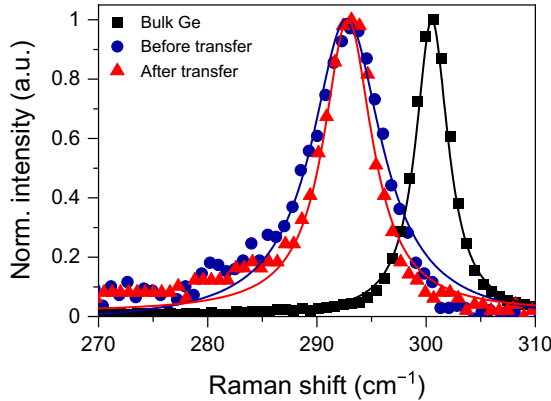
Note 5. Theoretical modeling of the gain and loss dynamics

References

Note 1. Nanowire transfer procedure

To transfer the as-grown nanowires onto the SiO₂ layer, we prepared an as-grown nanowire sample and an Si substrate coated with a thermally grown SiO₂ layer. We rubbed the as-grown nanowires directly against the oxidized Si substrate. The as-grown nanowires were then transferred onto the SiO₂ layer. During the transfer process, the nanowires were evenly distributed from low density to high density on the entire SiO₂ layer. We investigated an area where nanowires are sparsely distributed through an optical microscope and conducted experiments in the area where only one single nanowire can be optically pumped.

Note 2. Raman analysis on nanowires before and after transfer process

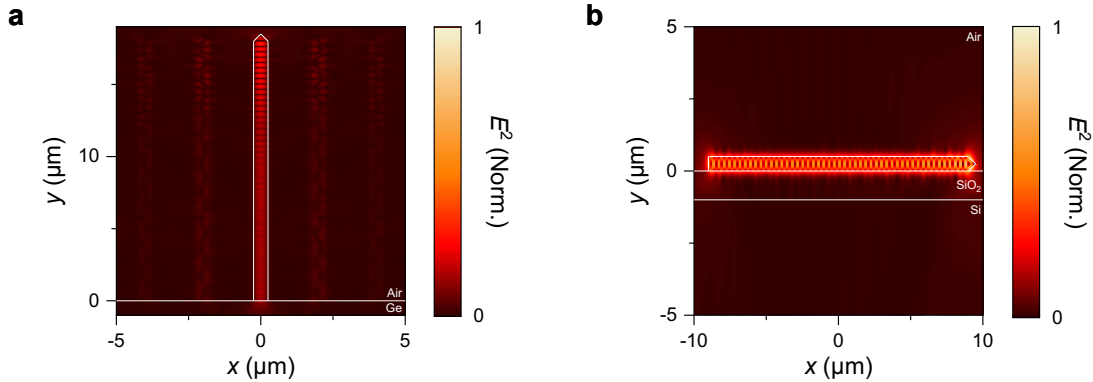


Supplementary Figure 1 | Raman characterization of as-grown and transferred nanowire samples.

Raman spectra of as-grown (blue curve) and transferred nanowire (red curve) samples showing peak positions of 292.7 and 292.8 cm⁻¹, respectively. A Raman spectrum of a bulk Ge (black curve) with a peak position of 300.5 cm⁻¹ is provided for reference. The single transferred nanowire shows a narrower FWHM of ~ 5.41 cm⁻¹ than that of as-grown nanowires (~ 7.79 cm⁻¹), indicating multiple nanowires being optically pumped simultaneously in the as-grown sample. The corresponding Sn content from the Raman peak position is calculated to be ~ 10 at.%.

To confirm that the transfer process does not induce any damage to the nanowires, we conducted the Raman spectroscopy measurement, which can assess defects and disorders in materials¹. Supplementary Figure 1 shows the measured Raman spectra of the as-grown vertically standing nanowires (blue curve) and a single transferred nanowire (red curve). A spectrum from bulk Ge (black curve) is also included as a reference. We confirmed that while the peak positions of the two samples are nearly consistent, the single transferred nanowire shows a narrower full-width at half-maximum (FWHM) of ~ 5.41 cm⁻¹ than that of as-grown vertical nanowires (~ 7.79 cm⁻¹). For as-grown vertical nanowires, approximately 3 nanowires are simultaneously excited by the 532-nm pump laser with a focused laser spot size of ~ 1 μ m. As each nanowire may have slightly different physical characteristics (e.g., Sn content, residual stress, physical dimension, etc.), the measured Raman spectra from multiple vertical nanowires can display a larger FWHM compared to a single transferred nanowire. From the Raman peak position, we can deduce an Sn content of ~ 10 at%, which is consistent with the Atom Probe Tomography (APT) result.

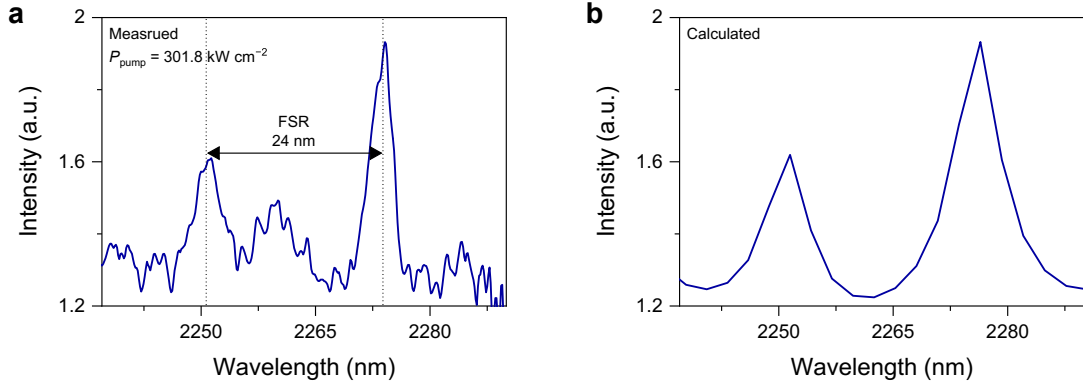
Note 3. Optical mode confinement of as-grown and transferred nanowires



Supplementary Figure 2 | Simulated optical mode profiles of as-grown and transferred nanowires. **a**, Cross-sectional mode profile of an as-grown nanowire, showing weak optical fields due to significant leakage of fields from the GeSn nanowire to the Ge substrate. **b**, Cross-sectional mode profile of a transferred nanowire, showing strong optical confinement due to large index contrast between a GeSn nanowire and an SiO_2 layer.

To investigate whether a transferred nanowire could confine the light better than an as-grown nanowire, we performed finite-difference time-domain (FDTD) optical simulations. The simulated wavelength is set to 2275 nm which is the peak wavelength of our resonance spectrum. GeSn (480 nm), Ge (20 nm) and Si with refractive indices of 4.3², 4.1 and 3.4, respectively, were employed for the as-grown nanowire simulation. For the transferred nanowire simulation, an SiO_2 with a refractive index of 1.44 is additionally employed above the Si substrate. Supplementary Figure 2a shows a simulated cross-sectional optical mode profile of the vertically standing as-grown nanowire. As shown in the Ge layer, there is a significant leakage of optical fields from the Ge/GeSn nanowire to the Ge substrate, thereby showing weak optical fields in the nanowire. The small refractive index contrast between the nanowire and the substrate causes the leakage of fields, hindering optical confinement in the nanowire. In stark contrast to a poor optical confinement in the as-grown nanowire, a nanowire transferred onto an SiO_2 layer shows strong optical confinement as shown in Supplementary Fig. 3b. The large refractive index difference between the Ge/GeSn nanowire and the SiO_2 layer prevents the leakage of fields from the nanowire to the Si substrate, enabling strong optical confinement in the nanowire.

Note 4. Comparison between simulated and experimental cavity resonances



Supplementary Figure 3 | Simulated and measured spectra of transferred nanowire. **a**, Magnified view of a spectrum experimentally measured at 120.7 kW cm^{-2} (black dashed line in Fig. 3a), showing two strong cavity resonances with an FSR of $\sim 24 \text{ nm}$. **b**, theoretical spectrum calculated by FDTD optical simulation, exhibiting a mode spacing of $\sim 25 \text{ nm}$. The experimental value corresponds to the calculated value, confirming that resonances are attributed to the longitudinal cavity in the nanowire.

To study whether the cavity resonances originate from the longitudinal modes in Ge/GeSn nanowire cavity, we compared the observed free spectral range (FSR) with a theoretical mode spacing calculated by FDTD optical simulation. Supplementary Figure 3a presents a magnified view of two strong cavity modes taken at 120.7 kW cm^{-2} (black dashed line in Fig. 3a), exhibiting an FSR of $\sim 24 \text{ nm}$. Supplementary Figure 3b shows two modes with a space of $\sim 25 \text{ nm}$ calculated by FDTD optical simulation. A simulated spectrum using FDTD simulation that is in excellent agreement with the experimental observation. The theoretically calculated value ($\sim 25 \text{ nm}$) corresponds to the experimentally measured value ($\sim 24 \text{ nm}$), thus confirming that resonances stem from the longitudinal cavity in the nanowire.

Note 5. Theoretical modeling of the gain and loss dynamics

The interband gain, and also the inter-valence band absorption, were calculated from the 8-band $\mathbf{k}\cdot\mathbf{p}$ model, using the expressions from Chuang *et al.*³. The Luttinger parameters of GeSn alloy are calculated according to Liu *et al.*⁴, and other parameters are listed in Rainko *et al.*⁵. To find the net gain, the free-carrier absorption can be calculated using the second order perturbation model described in Tsai *et al.*⁶, with the acoustic phonon, deformation potential (L-valley), intervalley, ionized impurity, and alloy scattering included. Alternatively, it can be calculated from expressions coming from fitting to experiment for Ge^{7,8}, and we have here used the later option. Finally, the indirect absorption (towards the L- and X-valleys in conduction band) which may be important in group-IV materials, was also included, as described in Virgilio *et al.* and Trupke *et al.*^{9,10}, but in this particular system it turned out to be negligible.

References

1. Gouadec, G. & Colombar, P. Raman Spectroscopy of nanomaterials: How spectra relate to disorder, particle size and mechanical properties. *Prog. Cryst. Growth Charact. Mater.* **53**, 1–56 (2007).
2. Tran, H. *et al.* Systematic study of $\text{Ge}_{1-x}\text{Sn}_x$ absorption coefficient and refractive index for the device applications of Si-based optoelectronics. *J. Appl. Phys.* **119**, 103106 (2016).
3. Chaung, S. L. *Physics of photonic devices*. (Wiley New York, 2009).
4. Liu, S.-Q. & Yen, S.-T. Extraction of eight-band $k \cdot p$ parameters from empirical pseudopotentials for GeSn. *J. Appl. Phys.* **125**, 245701 (2019).
5. Rainko, D. *et al.* Investigation of carrier confinement in direct bandgap GeSn/SiGeSn 2D and 0D heterostructures. *Sci. Rep.* **8**, 15557 (2018).
6. Chin-Yi Tsai *et al.* Theoretical model for intravalley and intervalley free-carrier absorption in semiconductor lasers: beyond the classical Drude model. *IEEE J. Quantum Electron.* **34**, 552–559 (1998).
7. Liu, J. *et al.* Tensile-strained, n-type Ge as a gain medium for monolithic laser integration on Si. *Opt. Express* **15**, 11272 (2007).
8. Peschka, D. *et al.* Modeling of Edge-Emitting Lasers Based on Tensile Strained Germanium Microstrips. *IEEE Photonics J.* **7**, 1–15 (2015).
9. Virgilio, M., Manganelli, C. L., Grosso, G., Pizzi, G. & Capellini, G. Radiative recombination and optical gain spectra in biaxially strained n -type germanium. *Phys. Rev. B* **87**, 235313 (2013).
10. Trupke, T., Green, M. A. & Würfel, P. Optical gain in materials with indirect transitions. *J. Appl. Phys.* **93**, 9058–9061 (2003).